

Anomalous localization effects associated with excess volume of cobalt catalyst in multiwalled carbon nanotubes

Junji Haruyama,^{a)} Izumi Takesue, and Tetsuro Hasegawa
Aoyama Gakuin University, 6-16-1 Chitosedai, Setagaya, Tokyo 157-8572, Japan

(Received 26 April 2002; accepted 8 August 2002)

We report on the anomalous localization effects strongly associated with excess volume of a cobalt catalyst in multiwalled carbon nanotubes (MWNTs) synthesized in nanoporous alumina membranes. These effects bring about the following anomalies in bulk MWNTs: (a) A slight increase in the volume of excess cobalt changes antilocalization (AL) to weak localization (WL), (b) a further increase in excess changes this WL back to the AL, but only in magnetoresistance (MR) oscillation, and (c) even under this AL in MR, AL can not be observed in the conductance versus logarithmic temperature relation. Mechanisms for these anomalies were discussed based on the unique MWNT structures. © 2002 American Institute of Physics. [DOI: 10.1063/1.1511535]

Carbon nanotube (CN), a molecular conductor, can be synthesized by a catalytic process using a ferromagnetic catalyst.¹ Because such catalysts remain in CNs even after the synthesis under excess catalyst volume, it is very interesting to clarify how the excess volume of ferromagnetic catalysts contributes to changes in the physical characteristics of CNs. The following two aspects can at least contribute to these: (a) during synthesis, excess volume changes CN structures, and (b) after synthesis, excess volume remaining in CNs play the role of magnetic impurities. No work has been reported on the first of these aspects, whereas the second aspect has been successfully studied in single-walled CN, implying efficient relaxation of the conducting electrons because of its large carrier mean-free path.^{2,3}

In contrast, the electrical properties of multiwalled CNs (MWNTs) are basically understood by the phase interference of quantum electron waves in the diffusive regime.^{4–10} A typical example is a two-dimensional (2D) weak localization (WL), a constructive phase interference. Here, the conductance (G) of 2D WL exhibits linearly logarithmic temperature ($\log[T]$) dependence with a saturation region forming at low temperatures. The $\log[T]$ -dependent region is a manifestation of decoherence by electron–phonon scattering, whereas the saturation region implies decoherence by spin–flip scattering due to magnetic impurities. MWNTs has also exhibited this 2D-WL behavior.^{4,6,7} The influence of magnetic impurities on the electrical properties of MWNTs has been reported in regard only to this decoherence for spin relaxation, including our past report.^{6,7} In this work, we reveal that such a spin interference in MWNTs is very sensitive to increases in excess cobalt catalysts with three anomalies and propose its application.

Figure 1(a) shows the schematic cross section of our MWNT array. Although we measured the physical properties of MWNTs as averaging about 10^3 in the array, it was already confirmed in Ref. 11 that the averaged properties were mostly the same as those of individual MWNTs. It also turned out that even such averaged measurement results could exhibit unique quantum-mesoscopic phenomena (see Refs. 6, 7, and 12). Figures 1(b)–1(d) stress unique struc-

tures depending on each excess cobalt deposition time. Such structures have been never observed in the sample with cobalt deposition time of 30 s.

Figure 2 reveals drastic changes in the G_0 versus $\log[T]$ relation, depending strongly on the deposition time. Figure 2(a) and its inset exhibit a slight decrease of G_0 as the temperature increases (i. e., negative G_0 behavior) up to $T=2$ K. In contrast, Fig. 2(b) interestingly implies that this decrease of G_0 disappears and only a saturation region emerges at the lowest temperatures. The further increase of the cobalt deposition time surprisingly leads to the elimination of this saturation region [Fig. 2(c)]. Even negative G_0 behavior is unobservable. At almost all of the temperatures measured, only a linear and positive G_0 versus $\log[T]$ relation appears.

The characteristics in Fig. 2 can be qualitatively understood as follows. Figure 2(a) results from the presence of “antilocalization” (AL), a destructive phase interference phenomenon, as we reported previously.¹² In that study, we revealed that the gold-diffusion region at the top end of our MWNTs had “spin–orbit interaction” (SOI) and the spins flipped by this SOI were injected into the bulk MWNT [Fig. 4(a)], leading to the phase shift by π and, hence, the AL. Decoherence of this AL due to the increased temperature leads to a negative G_0 versus $\log[T]$ relation [Fig. 2(a)] because the destructive interference is eliminated.

In contrast, qualitatively Fig. 2(b) means the emergence of 2D WL, consistent with previous reports on MWNTs,⁴ with magnetic-impurity (spin–flip) scattering at low temperatures. Quantitatively, the relation was well fitted by the following formula of 2D WL⁶ [the solid line in Fig. 2(b)]. The T_c a transition temperature between dephasing regimes due to electron–phonon scattering and spin–flip scattering, as high as 5.4 K, obtained from the best fitting, actually stresses the presence of strong spin–flip scattering due to magnetic impurities. In contrast, the best fitting to Fig. 2(c) gives T_c as low as 1.7 K, which actually emphasizes a mostly linear G_0 versus $\log[T]$ relation in the measured temperature range.

In order to confirm these AL and 2D WL, we measured the magnetoresistances (MRs) in the sample in each figure (Fig. 3). Figure 3(a) emphasizes a positive MR around $B=0$ T. This is qualitatively consistent with decoherence of the AL

^{a)}Electronic mail: j-haru@ee.aoyama.ac.jp

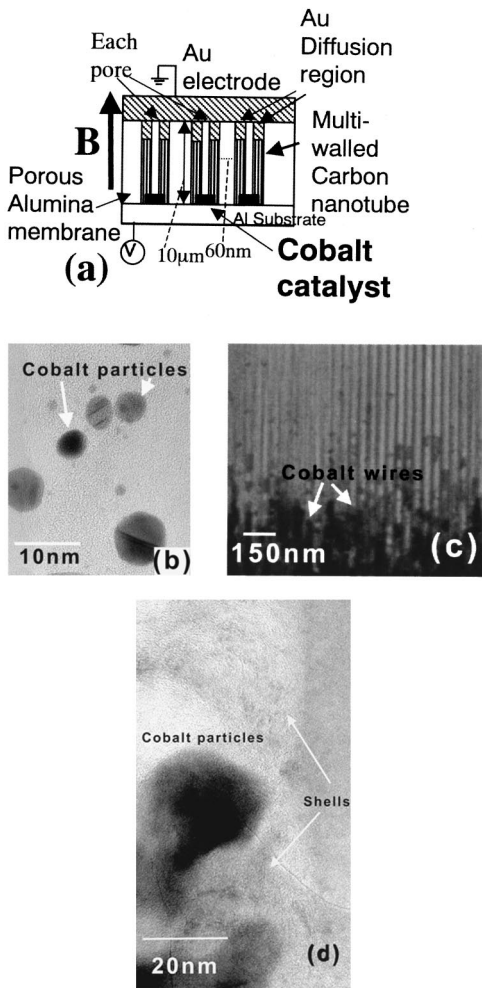


FIG. 1. (a) Schematic cross section of an MWNT array, synthesized into nanopores of alumina membranes, using cobalt catalyst (see Refs. 6, 7, and 12). We prepared three samples with three different times for the cobalt deposition, i. e., 30, 120, and 360 s. The deposition time of 30 s corresponds to the optimal cobalt volume, whereas 120 and 360 s lead to the slightly and highly excess cobalt volumes, respectively. (b) and (c): Cross-sectional transmission electron microscopy (CRTEM) images of the samples with “30 s” cobalt deposition. (b) The cobalt particles without any shells, included in the MWNT, (c) The short cobalt wires formed at the bottom of MWNTs, and (d) CRTEM image of the samples with “360 s” deposition time. This implies the cobalt-particle arrays surrounded by the highly disordered (a coffee-cup structure) and thick shells.

[Fig. 2(a)]. In contrast, a negative MR surprisingly emerges around $B=0$ T in Fig. 3(b). This is also qualitatively consistent with decoherence of the 2D WL shown in Fig. 2(b).

For quantitative confirmation, we performed data fitting for Figs. 3(a) and 3(b) by the revised Altshuler’s formulas for Altshuler–Aronov–Spivak (AAS) oscillation as used in our past works.¹² In the formula, whether either negative or positive MR emerges around zero magnetic field (i. e., either WL or AL) is decided by the terms of $(L_\varphi/L'_\varphi)^2 = 1 + 2(L_\varphi^2/D\tau_{so})$, where L_φ , L'_φ , τ_{so} , and D are the phase coherent length without and with SOI, the relaxation times for SOI, and the diffusion constant, respectively. In this equation, infinite τ_{so} leads to $(L_\varphi/L'_\varphi) = 1$, corresponding to WL. In contrast, finite τ_{so} leads to $(L_\varphi/L'_\varphi)^2 > 1$, resulting in AL due to SOI. We can identify L_φ and L'_φ , using this L_φ/L'_φ as the fitting parameter.

The agreement between data and theory is good in each figure, also for the bimodal oscillations (i. e., lines A and B).

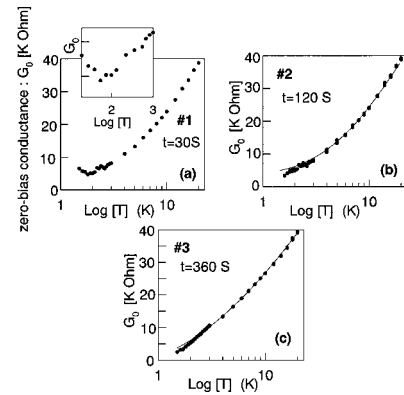


FIG. 2. Zero-bias conductance (G_0) vs logarithmic temperature ($\log[T]$) relations in the samples with the three different cobalt-deposition times. Solid lines are the calculation results by 2D WL formula for MWNTs (see Ref. 6).

This bimodal behavior means the presence of two different L_φ/L'_φ . Because L_φ/L'_φ depended on the diffusion volume of gold atoms [Fig. 4(a)], we clarified that this bimodal behavior was attributable to the presence of two distribution peak of this gold-diffusion volume in one array.¹² Here, because the best fitting to the line A in Fig. 3(a) gives $[L_\varphi/L'_\varphi = 10.2 \mu\text{m}/1.1 \mu\text{m}] > 1$, this means the finite value of τ_{so} and, hence, quantitatively supports the presence of AL in Fig. 2(a). In contrast, because the best fitting to Fig. 3(b) gives $[L_\varphi/L'_\varphi = 1.12 \mu\text{m}/1.02 \mu\text{m}] \sim 1$, this is also consistent with the presence of 2D WL in Fig. 2(b).

In Fig. 3(c), a positive MR surprisingly emerges again with the bimodal oscillations. The best fitting to line A gives $[L_\varphi/L'_\varphi = 8.2 \mu\text{m}/0.75 \mu\text{m}] > 1$, implying the presence of AL, similar to Fig. 3(a). One should note that this is “not” consistent with the linear G_0 versus $\log[T]$ relation shown in Fig. 2(c), because AL should exhibit a negative G_0 versus $\log[T]$ relation like Fig. 2(a).

Consequently, we confirm that Figs. 2 and 3 emphasize the emergence of AL and WL strongly depending on the volume of excess cobalt, by following three anomalies: (a) a slight increase in the excess cobalt volume caused a transition from the AL to the 2D WL, (b) a further increase changed this WL back to the AL only in the MRs, and (c) despite that, AL was unobservable in the G_0 versus $\log[T]$

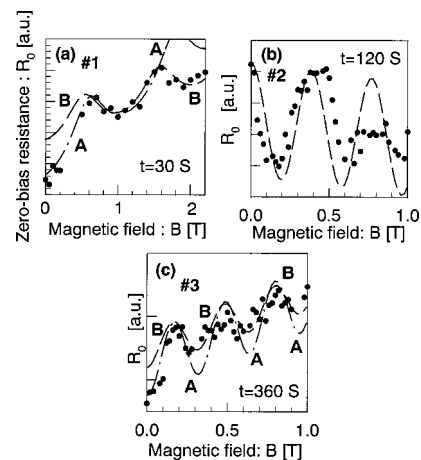


FIG. 3. Dependence of MR features, corresponding to each figure in Fig. 2. A magnetic field was applied along the tube axis. Lines A and B in (a) and (c), and the dotted line in (b) are the calculation results by the revised formula of AAS oscillation. (see Ref. 12).

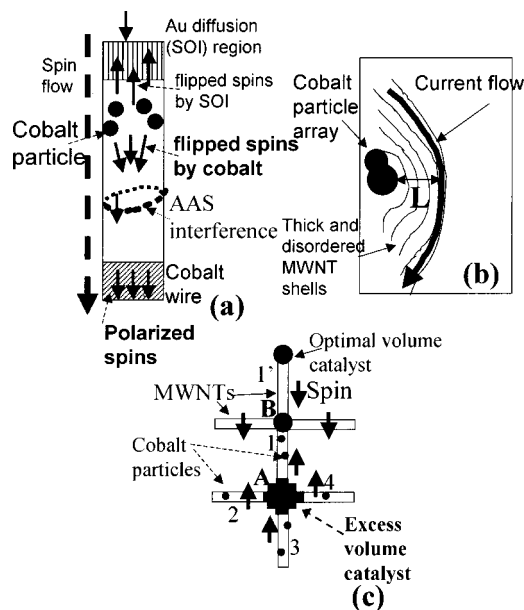


FIG. 4. Schematic cross sections of the MWNTs (a) for Figs. 1(b) and 1(c), and (b) for Fig. 1(d), and (c): The MWNT networks formed by ferromagnetic catalyst networks.

dependence, exhibiting only the linear $\log[T]$ relation. We propose the following interpretation for these, based on Figs. 1(b)–1(d).

The first anomaly can be qualitatively interpreted as follows. We found many cobalt particles remaining in the MWNTs of the Figs. 2(b) and 3(b) sample [Fig. 1(b)]. If the spin flipped by the SOI at the top of MWNT is flipped by these cobalt particles in the n th time (here, n should be the odd integer) during flowing through the MWNT before AAS interference occurs, the interference is caused by this flipped spin with opposite moment. Because this leads to a phase shift by π in the AAS interference [Fig. 4(a)], this changes the AL to the WL. The flipped spins, however, remain strong fluctuation. After the AAS interference occurred, spins with such fluctuation are injected into the short cobalt wire at the bottom end of MWNT [Fig. 1(c)]. If this cobalt nanowire plays a role of spin polarization for these spins, all of such spins will be aligned losing the fluctuation during flowing through this cobalt nanowire [Fig. 4(a)]. In fact, it was reported that MWNTs connected to ferromagnetic electrodes exhibited strong spin polarization.⁹ Consequently, the clear WL appears in Figs. 2(b) and 3(b), when the magnitude of this WL becomes dominant compared with that for the AL.

Quantitatively, in this case, “SOI length (L_{so})” \geq “spin scattering length (L_s)” has also been confirmed.

The second anomaly can be qualitatively interpreted by Fig. 1(d). In Fig. 1(d), we found (a) the cobalt particles were combined into cobalt-particle arrays, and (b). Such cobalt-particle arrays were surrounded by the disordered and thick shells of the MWNTs. These can be yielded by the extremely high density of cobalt particles, due to a further increase in the excess volume of the cobalt catalyst that is far from the optimal condition, in the MWNT. Here, because electron waves in our MWNTs flow along the outer portions of the shells,¹² these thick shells increase L in Fig. 4(b), reducing the influence of spin-flip scattering due to the cobalt particles [Fig. 4(b)]. This leads to the elimination of the 2D WL,

because the origin for the 2D WL in Fig. 3(b) was this spin-flip scattering. This in turn changes the WL back to the AL. “ $L_\phi > L'_\phi$ ” obtained from the data fitting quantitatively supports this explanation, because only L_s can increase in this structure, along with decreased L_{in} as mentioned next.

In contrast, the third anomaly stresses decoherence by only strong electron-phonon scattering. The highly disordered shell structure observed in Fig. 1(d) emphasizes the possible presence of strong electron-phonon scattering in this MWNT (i.e., a decrease of L_{in}), leading to the elimination of AL. Besides, dephasing by the cobalt particles leading to the low-temperature saturation in the WL is also reduced by the thick shells as previously mentioned. Therefore, only the lineal and positive G_0 versus $\log[T]$ relation can emerge [Fig. 2(c)]. This behavior, however, can be consistent with the AL in MR [Fig. 3(c)], because (a) the positive MR in Fig. 3(c) was yielded by decoherence of SOI due to the increase of magnetic field at the fixed temperature ($T=1.5$ K), whereas the third anomaly is caused by decoherence of electron-phonon interaction due to the increase of temperature at the fixed magnetic field ($B=0$), and (b) decoherence of SOI and electron-phonon scattering are very sensitive only to magnetic field and temperature, respectively. These second and third anomalies stress that the thick shell of MWNTs reduces the influence of spin-flip scattering under the magnetic-filled change, but its disorder enhances the electron-phonon interaction under the temperature change.

Individually, all of these three anomalies can be universal in MWNTs by virtue of the strong spin coherence. The coexistence of the second and third anomalies, however, may be not universal, because it can be constructed only under balance of some structural conditions.

Finally, based on these effects, we briefly propose spin moment switching in MWNT networks fabricated by ferromagnetic catalyst networks [Fig. 4(c)].¹ One can flip the spin moment only in the MWNTs (1–4) in Figs. 4(a). This will promise spin ironics circuits because the phenomena reported here are reproducible.

The authors thank B. Altshuler, M. Dresselhaus, and Ph. Avouris for their useful discussions and encouragement. This work has been supported both by a Grant-in-Aid for research projects and by the “Carbon Nanotube Electronics” project from the Special Coordination Funds for Promoting Science and Technology by Japanese Government, and by the MST.

¹H. Dai, in *Carbon Nanotubes*, edited by Mildred and Gene Dresselhaus (Springer, Berlin, 2001), p. 29.

²L. Forro and C. Schonenberger, in *Carbon Nanotubes*, edited by Mildred and Gene Dresselhaus (Springer, Berlin, 2001), p. 329.

³T. W. Odom, J.-L. Huang, C. L. Cheung, and C. M. Lieber, *Science* **290**, 1549 (2000).

⁴L. Langer, V. Bayot *et al.*, *Phys. Rev. Lett.* **76**, 479 (1996).

⁵Bachtold, C. Strunk *et al.*, *Nature (London)* **397**, 673 (1999).

⁶J. Haruyama, I. Takesue, T. Hasegawa, and Y. Sato, *Phys. Rev. B* **63**, 073406 (2001).

⁷J. Haruyama, I. Takesue, and Y. Sato, *Appl. Phys. Lett.* **77**, 2891 (2000).

⁸T. W. Ebbesen, H. J. Lezec, H. Hiura *et al.*, *Nature (London)* **382**, 54 (1996).

⁹K. Tsukagoshi, B. W. Alphenaar *et al.*, *Nature (London)* **401**, 572 (1999).

¹⁰H. R. Shea, R. Martel, and P. Avouris, *Phys. Rev. Lett.* **84**, 4441 (2000).

¹¹C. Papadopoulos, J. M. Xu *et al.*, *Phys. Rev. Lett.* **85**, 3476 (2000).

¹²J. Haruyama, I. Takesue, and T. Hasegawa, *Appl. Phys. Lett.* **79**, 269 (2001); *Phys. Rev. B* **65**, 33402 (2002).